

Biological Single Molecule Applications and Advanced Biosensing

M. Hegner^{a,*}, Ch. Gerber^{a, b}, Y. Arntz^a, J. Zhang^a, P. Bertoncini^a, S. Husale^a, H.P. Lang^{a, b} and W. Grange^a

^aInstitute of Physics, NCCR Nanoscale Science, University of Basel
Klingelbergstrasse 82, CH - 4056 Basel, Switzerland

^bIBM Zurich Research Laboratory, Säumerstrasse 4, CH- 8803 Rüschlikon,
Switzerland

*Corresponding author: martin.hegner@unibas.ch

1. INTRODUCTION

1.1. Macroscopic versus microscopic measurements in biology

Macroscopic experiments yield time and population averages of the individual characteristics of each molecule. At the level of the individual molecules, the picture is quite different: individual molecules are found in states far from the mean population, and their instantaneous dynamics are seemingly random. Whenever unusual states or the rapid, random motions of a molecule are important, the macroscopic picture fails, and a microscopic description becomes necessary. Single-molecule experiments differ from macroscopic measurements in two fundamental ways: first, in the importance of the fluctuations in both the system and in the measuring instrument, and second, in the relative importance of force and displacement as variables under experimental control and subject to direct experimental measurements. In single-molecule experiments, the crucial parts of the measuring instruments themselves are small and subject to the same fluctuations as the system under study. Single-molecule experiments thus, give access to some of the microscopic dynamics that are hidden in the macroscopic experiments.

1.2. Force sensitive Methods

During the last decade, new force measuring devices have been developed which paved the way to explore the rich possibilities of mechanical measurements in the Pico Newton (pN) range of force generating motor-proteins and interacting biological macromolecules under physiological conditions.

One of them is the optical trapping scheme, which consists of bringing a beam of laser light to a diffraction-limited focus using a “good” lens, such as a microscope objective. Under the right conditions, the intense light gradient near

the focal region can achieve stable three-dimensional trapping of dielectric objects, varying in size from a few tens of nanometers up to tens of micrometers. The term optical tweezers (OT) was defined to describe this so called single-beam scheme.

Another force-measuring device is the scanning force microscope (SFM), which has evolved to a unique tool for the characterization of organic and biological molecules on surfaces. The SFM has proven its impact for biological applications, showing that it is possible to achieve sub nanometer lateral resolution on native membrane proteins in buffer solutions [1], to monitor enzymatic activity *in situ* [2] or to measure the unfolding of single proteins [3]. Up to now there is plenty of experimental information available regarding forces, which arise in biological systems. An overview upon force-measuring experiments carried out during the last few years to get information on biological systems is shown in figure 1.

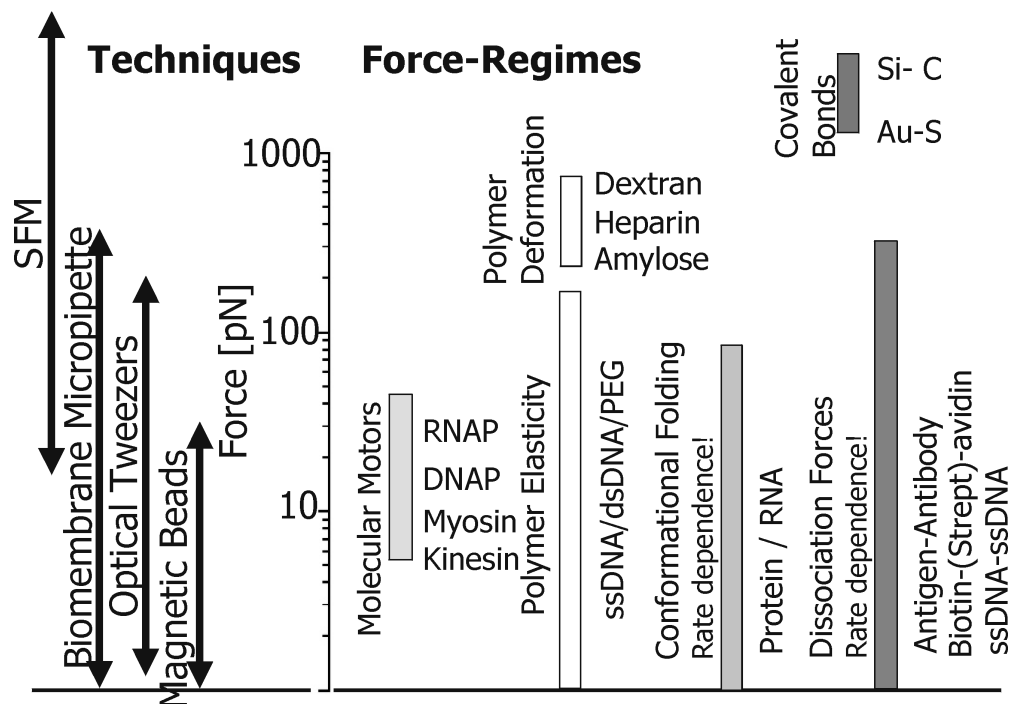


Figure 1: Overview on techniques, which are applied to assess information upon forces in biological systems. On the right a series of experiments in the various areas of motors proteins or molecular mechanics are shown. Some of the experiments like unfolding of individual proteins and dissociating (bio-molecular) bonds depend on the rate of the applied external force.

There is complementary biological information gathered by the various techniques. As visible in the graph, the force regime in which optical tweezers and scanning force microscopy are used overlap nicely. Optical tweezers preferably are applied in experiments on molecular motors and entropic elasticity of molecules and conformational folding of proteins and rupturing of bonds are mainly investigated by SFM.

In addition it has been shown during the last few years that the interaction of biomolecules on interfaces can be used as a tool for biosensing. The signal of the interaction of biomolecules on specific ‘receptor’ interfaces is transduced into a nanomechanical motion that is easily detected by the cantilever array technique a specific method evolved from the scanning force microscopy. It is the purpose of this review to give an insight into these fields of our research activities in the Physics Institute at the University of Basel.

2. OPTICAL TWEEZERS

As mentioned previously, optical tweezers (OT) are instruments, which allow to trap or levitate micron-sized dielectric particles using laser light. In addition, minute forces can be measured on the trapped particles with accuracy much better than what can be achieved with scanning force microscopy (in liquid and at room temperature). This explains why OT is nowadays considered as a technique of choice for the investigation of biomechanical forces. This section aims to give a basic introduction on this single-molecule technique (a single molecule can be attached to the handle and therefore its mechanical properties can be studied), describing technical details and possible implementation and calibration of OT instruments. Moreover, typical experiments performed with OTs will be highlighted.

2.1. Origin of Optical Forces

It was first demonstrated in 1970 by Ashkin that light could be used to trap and accelerate dielectric micron-sized particles [4]. For this experiment, a stable optical potential well was formed using two slightly divergent counter-propagating laser beams. This pioneer study established the groundwork for the Optical Tweezers (OT) technique, where a single laser beam is focused by a high numerical aperture (NA) objective lens to a diffraction-limited spot [5]. At the focus, not only dielectric particles spheres can be trapped but also biological organisms such as cells, virus, or bacteria [6, 7]. Although it is still challenging for theory to calculate typical optical forces [8, 9], the origin of optical forces can be understood easily (Fig. 2). Since a bundle of light rays is refracted when passing through a dielectric object, existing rays have a different directions than incoming rays. This results in the change in light momentum. By conservation of momentum, the change in the light momentum causes a change ΔP in the momentum of the trapped particle. As a result and due to Newton's second Law, the particle will feel a force F :

$$F = \frac{\Delta P}{\Delta t} = \frac{nQW}{c} \quad (1)$$

where n is the index of refraction of the surrounding medium, W the power of the laser, c the celerity of the light, and Q is a dimensionless factor, known as the trapping efficiency.

Optical forces are however very small, since 100 mW of power at the focus (10^{+7} W/cm²) produces forces of only a few tens of pN on a micron-sized particle.

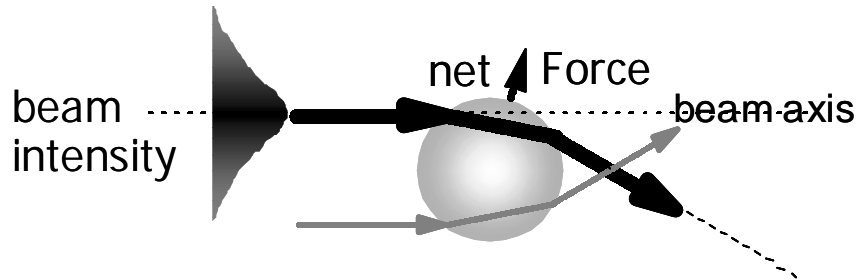


Figure 2: A transparent dielectric micron-sized particle with an index of refraction larger than the surrounding medium is pushed towards the largest intensity of the light. All light rays are refracted when entering the particle. Due to second Newton's law, the change in light momentum flux (the force) causes a reaction force on the particle. Center rays contain more photons than outer rays and exert therefore more force. The resulting net force is shown.

For biological applications, it is therefore imperative to choose a laser excitation, which (i) does not rise the temperature of the surrounding medium (say water) and (ii) prevents biological damage. It has been shown that near infrared excitation is always best suited, although the wavelength region between 700 and 760 nm should be avoided in typical OT experiments [10, 11].

As seen above, light exerts a pressure on dielectric particles. For practical applications, we need however to form a stable optical trap. In a simple picture, it can be shown that a stable trapping occurs when the scattering force is smaller than the gradient force. Basically, the scattering force (due to Fresnel reflections at the surface of the dielectric particle) is proportional to the power of the laser and acts only in the direction of propagation. As a consequence, this force does not trap. In contrast, the gradient force (proportional to the spatial gradient of the light) arises whenever the particle is out of the beam axis. This force acts therefore in 3-dimensions and tends to pull the particle towards the region of maximum spatial gradient (*i.e.* the focal point) if the index of refraction of the particle is larger than that of the buffer solution. This simple picture explains why a stable trapping is observed only when (i) high NA objective lenses are used (ii) the back aperture of the objective lens has to be overfilled (to produce a diffraction limited spot and therefore a maximum spatial gradient). Moreover, it suggests that handles with high refractive index (at least larger than the surrounding medium) have to be used.

2.2. Experimental Details

Knowing the origin of optical forces, we can build an optical trap. In principle, the design of such instruments should be easy since trapping requires only (i) a beam expander to overfill the back aperture of the microscope lens (ii) a good microscope lens with a high NA to produce a steep spatial gradient (iii) in addition when biological research is the focus of the experiment, lasers using wavelength in the near infrared should be used to avoid damage on the biological matter. Indeed, some rather simple modifications of a commercial inverted microscope are sufficient to build an OT [12]. Of course, whenever the following requirements have to be considered (beam steering, high mechanical stability, proper spatial filtering of the laser, reducing mode hopping the laser...), it is best to build an OT on a conventional optical table with custom optics and electronics [8]. Note finally that oil immersion microscope lenses are less suited for OTs due to the difference in index of refraction between oil and water (inside the chamber). The major microscope providers have nowadays a high numerical water-immersion lens in their program, which circumvent this drawback.

2.2.1. Calibration procedure

One of the main difficulties in OT experiments is to correctly estimate the force that acts on the trapped particle. We already have mentioned that an object changes the direction of the refracted rays when it experiences a force. In principle, such a change in the light momentum flux can be easily monitored onto a position sensitive detector (PSD) if we place after the objective lens a condenser lens (Fig. 3).

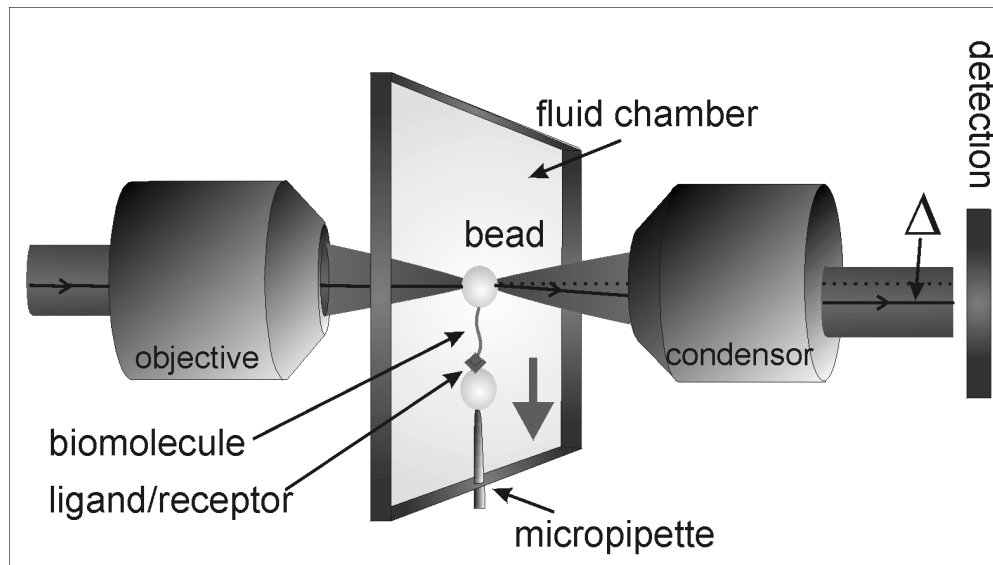


Figure 3: Schematic representation of an OT experiment. A microscope objective lens with a high NA is used to focus the laser light to a diffraction-limited spot. At the focus, where the spatial gradient is maximal, particle such as beads can be trapped. Light is collected with a condenser lens, which converts angular deflections into transverse deflections that can be monitored on a PSD. A single molecule can be attached between the trapped bead and a bead on a micropipette through a

receptor-ligand bridge. Mechanical properties of single molecules can be therefore investigated if the micropipette is placed onto a piezoelectric element. When the trapped bead experiences the force (arrow), it moves slightly away from its stable position. As in SFM, this leads to a deflection on the detector.

To relate deflections observed on the detector to forces, we need to calibrate the instrument. Many different approaches have been proposed in the past to perform such a calibration [8]. However, the thermal fluctuations calibration method is certainly the most widely used. Having an object in the trap, the stiffness K of the light lever can be estimated from the power spectral density $S(f)$ of the displacement fluctuations, using:

$$S(f) = \frac{k_B T}{\pi^2 \gamma (f^2 + f_c^2)} \times A^2 \quad (2)$$

where γ denotes the viscous drag, $f_c = K(2\pi\gamma)^{-1}$ is the corner frequency (*i.e.* the frequency above which the particle does not feel the effect of the trap anymore), $k_B T = 4.1$ pN·nm at room temperature, and A is a factor describing the sensitivity of the detector ($\text{V}\cdot\text{nm}^{-1}$). Fitting the measured power spectral density with Eq. (2) gives a robust estimate of the corner frequency and consequently of the trap stiffness if the viscous drag is computable (*i.e.* for an object of known shape).

In addition, the detector sensitivity can be obtained from the area under the spectral density curve, knowing that the mean square displacement of the particle is related to both $S(f)$ and K through:

$$\langle x^2 \rangle = \int S(f) df = \frac{k_B T}{K} \times A^2 \quad (3)$$

Such a procedure shows that both the trap stiffness and the detector sensitivity (which are the only parameters needed to estimate the force) can be determined from a detector that is not absolutely calibrated.

2.2.2. State of the art instrumentation

In the previous section, we have seen that single beam OTs can easily measure forces. However, an important drawback of such instruments is that a new calibration has to be performed for each new experiment (each time some local parameters such as the shape or size of the trapped particle, the local fluid viscosity, or power of the laser are changed). Indeed, single beam OTs do not directly measure the change in light momentum flux because of the scattering at the interface of the microscope lens that introduces marginal rays. As shown by Smith [13], dual beam OTs overcome such limitations. Such instruments, although more expensive and more expensive than single beam OTs, need to be calibrated only once and have a very high trapping efficiency, which is of prime importance for biological investigations [14].

2.2.3. Thermal noise

At room temperature, Brownian motion of the trapped particle (OT) or the cantilever (SFM) limits the force resolution of this micromechanical experiments. As seen in the previous section, the power spectral density (*i.e.* thermal noise) is constant for frequency below the corner frequency and rolls off rapidly for frequency above f_c . However, $S(f)$ usually extends to high frequencies. When the bandwidth f_s of the measurement is much smaller than the corner frequency or when low-pass filters are used, the minimum detectable force F_{min} reads (see Eq. (2) and (3)):

$$F_{min} = (K / A) \sqrt{\langle x^2 \rangle} = \sqrt{4\gamma k_B T f_s} \quad (4)$$

In this case, the force resolution is independent of the trap stiffness [15]. To improve the sensitivity of micromechanical experiments, we can decrease (i) the temperature, (ii) the bandwidth of our measurement, or (iii) the drag viscosity. Alternatively, the resonance frequency of the SFM cantilever can be increased to reduce the noise at a give bandwidth. Certainly the best approach is to decrease the drag viscosity by reducing the size of the force-sensing device (the trapped bead or the cantilever) [15, 16]. This explains the need for small SFM cantilevers when high force sensitivity has to be achieved. Note that commercial SFM cantilevers have typical dimensions of 100 μm , whereas beads used for OT experiments have diameters of the order of 1 μm . For this reason, the force noise level of OT measurements (below 0.3 pN) is much smaller than that of SFM based techniques (10 pN, in liquid and at room temperature). However, the maximum force that can be measured with OTs is rather small as compared to SFM based techniques. For instance, dual beam OTs can measure forces only up to 200 pN [14].

2.3. Recent experiments

We do not attempt to give an exhaustive review of all experiments that have been performed with OTs (see [17, 18] for recent reviews). Rather, we would like to select and describe briefly typical applications of OTs in biology.

2.3.1. Molecular motors

Certainly, one of the most impressive applications of OTs is the study of molecular motors on a single molecule level. These molecular motors can be linear motors (Kinesin, Myosin) [19], DNA/RNA polymerase enzymes [20, 21] or DNA packaging viruses (bacteriophage $\phi 29$) [22].

Kinesin and Myosin are two ATPase motor proteins. Kinesin, which is used for organelle transport or chromosome segregation, moves along microtubules. In contrast, Myosin interacts with actin filaments and is used not only for muscle contraction but also is involved in many forms of cell movement. For these studies, OTs are used to interact single Kinesin or Myosin

in vitro with either a microtubule or an actin filament (Fig. 4.A). These experiments have revealed how much ATP has to be hydrolyzed and the forces generated at each step, demonstrating possible mechanisms involved in the movement.

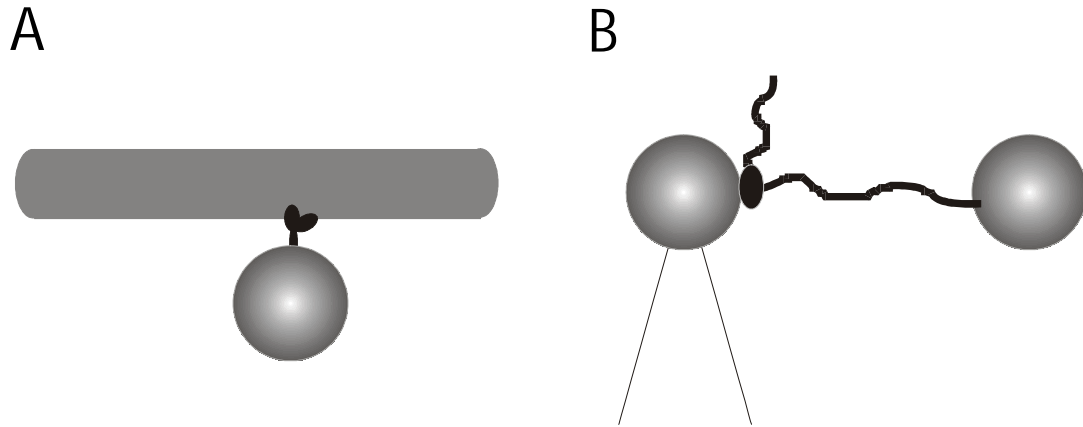


Figure 4: Possible experimental setups used for single molecule observation of molecular motors. (A) Beads coated with either Kinesin or Myosin are approached in the vicinity of a microtubule or an actin filament. For Kinesin studies, the microtubule is placed on a surface and the bead is held by the OT. Kinesin can walk continuously for long distances (microns) before being released from the microtubule. In contrast, Myosin only binds weakly to actin and is released after a one step movement. For these experiments, the bead has therefore to be immobilized onto a surface and an actin filament is stretched and held by two optical traps. (B) A bead coated with an enzyme (black) interacting with a DNA molecule is held by suction on top of a micropipette in a continuous flow of buffer solution. A bead coated with a receptor recognizing the ligand-modified DNA molecule end is approached till the end is connected through the biomolecular interaction of the receptor with the ligand using OT. The enzyme runs then along the single DNA molecule and is used either to transcribe a dsDNA template into a messenger RNA (RNA polymerase) or to incorporate base pairs on ssDNA (DNA polymerase).

Other experiments investigated the function of motor enzymes used in DNA transcription or DNA polymerization. In this case a single DNA molecule is tethered between two beads (Fig. 4.B), and the rate of transcription or polymerization can be followed in real time by applying a constant tension (force feedback) and allowing the distance between the beads to change accordingly. Such studies have direct implications for the mechanism of gene regulation or force-induced exonuclease activity.

2.3.2. Mechanical properties of single molecules

Due to the high force sensitivity, OTs have been used to study (i) mechanical properties of DNA [23] (ii) protein or RNA unfolding [24-26] (iii) the polymerization of individual RecA-DNA filaments [27]. Again, these experiments provided new insights in biochemical processes on a single molecule and are of great relevance to biology. In a recent publication Husale et al. [28] showed that optical tweezers can easily be applied to investigate the influence of small ligands directly interacting with DNA to elucidate the binding mechanism of the ligands on the DNA.

3. SCANNING FORCE SPECTROSCOPY

3.1. Introduction to Dynamic Force Spectroscopy

It has long been known that only molecules with an excess of energy over the average energy of the population can participate in chemical reactions. Accordingly, reactions between ligands and receptors follow pathways (in a virtual energy landscape) that involve the formation of some type of high-energy transition states whose accessibility along a reaction coordinate ultimately controls the rate of the reaction. Until recently, chemists and biologists could only act on molecules if these were present in large quantities. Consequently, scientists could only access macroscopic thermodynamical quantities, e.g. the free energy of complex formation and/or dissociation.

Today, instruments offering a high spatial resolution and sensitivity down to the Pico- or Femto-Newton range allow one to study the adhesion of molecular bonds [29-41]. In particular, a novel type of force spectroscopy, the so-called dynamic force microscopy (DFS), has been developed. In figure 5 a setup of a scanning force microscope used for dynamic force spectroscopy is shown.

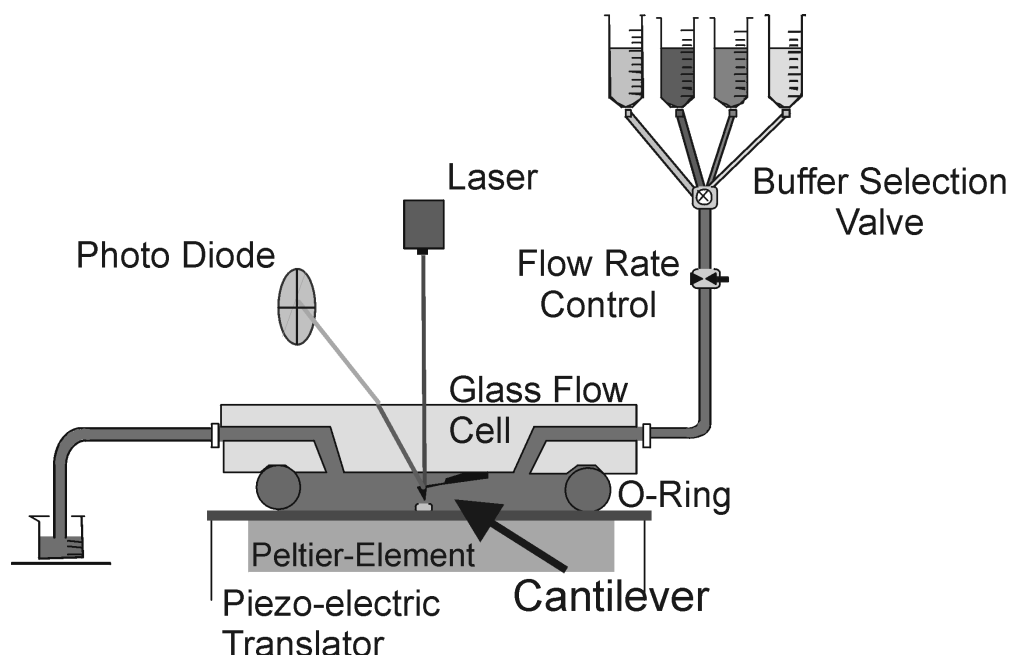


Figure 5: Setup of a scanning force microscope. The instrument is working in buffer media under ambient condition. A springboard type cantilever (dimensions $\sim 300 \times 20 \times 0.5 \mu\text{m}$, spring constant 0.01 N/m) is deflected when adhesive forces in-between the ligand-modified tip and the receptor-modified interface arises during retraction of the sample surface. The motion of deflection of the cantilever is detected using a laser beam, which is mirrored on the levers backside and projected onto a four-quadrant photosensitive diode. Various liquids can be injected and a peltier-element allows varying the temperature precisely.

In a DFS experiment, the dependence of the rupture force on the loading rate is investigated using a scanning force microscope (SFM), a bio-membrane

force probe (BFP), or eventually an optical tweezers setup. A rather detailed description of such experiments performed in our laboratory is given in this section [39-42]. For a typical DFS experiment using an SFM, a ligand is immobilized on a sharp tip attached to a micro-fabricated cantilever and the receptor is immobilized on a surface. When approaching the surface of the tip a bond may form between ligand and receptor. The bond is then loaded with an increasing force when retracting the surface from the tip. From these measurements, the energy landscape of a single bond can be mapped [43]. A typical force distance plot of these experiments is shown in figure 6.

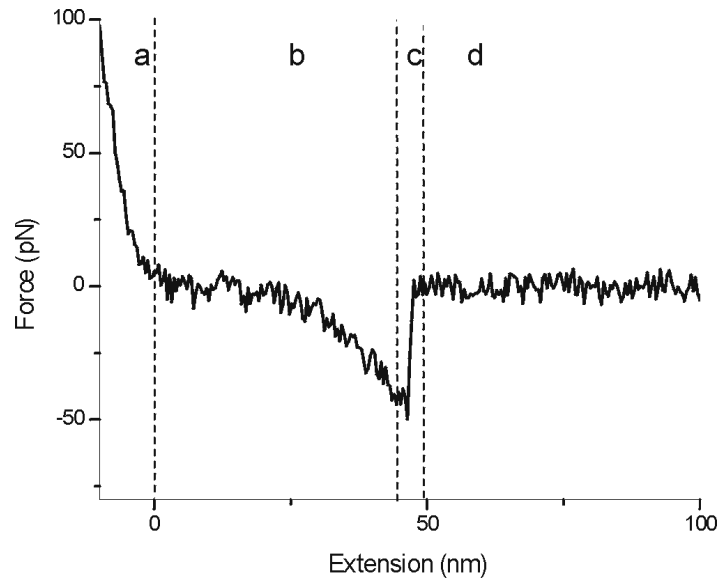


Figure 6: A typical force-distance curve obtained in a stretching SFM experiment (retraction cycle). A DNA strand (TATTAATATCAAGTTG) is immobilized by its 5'-end *via* a PEG linker on the SFM tip and its complement is attached in a similar fashion by its 5'-end to the surface. When the tip is approached close to the surface a specific bond between the two strands is formed (a). The SFM tip is then retracted from the surface at constant loading rate (b-[PEG stretching]). The sudden drop in the force curve reflects unbinding of the duplex (c-[specific DNA unbinding]). The loading rate r (retract velocity v times the elasticity c) is determined from the slope of the force-displacement curve before the unbinding event occurs.

This section is organized as follows. Part one introduces theoretical models that describe a chemical reaction when an external force is used to rupture a complex. Then, DFS experiments on complementary DNA strands are presented and illustrate the main ideas developed in part 3.1.

3.2. Theoretical Background

In this section, some thermo-dynamical models describing the rupture of a single bond will be briefly presented. More details can be found elsewhere [44-47].

Bell [45] first stated that the bond lifetime τ of an energy barrier reads:

$$\tau(F) = \tau_0 \exp[(E_0 - \Delta x F) / k_B T] \quad (5)$$

where T is the temperature, E_0 represents the bond energy (the height of the barrier), F is the external applied force per bond, Δx is the distance (projected along the direction of the applied force) between the ground state and the energy barrier (with energy E_0), and τ_0 is a pre-factor. Eq. (5) states that (i) a bond will rupture after a certain amount of time thanks to thermal fluctuations (ii) application of an external force dramatically changes the time it takes to overcome the energy barrier. Note finally that (5) can be re-written as:

$$k_{off}(F) = k_{off} \exp(F / F^0) \quad (6)$$

where k_{off} is the thermal off-rate of the barrier, and F^0 is a force-scale factor ($F^0 = k_B T / \Delta x$).

An important point is that the most probable force F^* needed to overcome an energy barrier should *a priori* depend on the loading rate, *i.e.* the velocity in a typical DFS experiment (typical values for velocities are in the range between 10 nm/s and 5000 nm/s). Indeed, when the loading rate decreases, F^* should decrease because of thermal fluctuations. In fact, a simple relation holds between F^* and the loading rate r ($r = kv$, where k is the stiffness of the DFS force sensor and v is the retraction speed):

$$F^* = F^0 \ln(r / F^0 k_{off}) \quad (7)$$

By plotting F^* as a function of $\ln(r)$, one should therefore find different linear regimes, each of them corresponding to a specific region (a specific energy barrier) of the energy landscape. According to Evans [46], the kinetics runs as follows: application of an external force (i) selects a specific path (a reaction coordinate) in the energy landscape (ii) suppresses outer barriers (Eq. 5), and reveal inner barriers which start to govern the process. For instance, recent BFP and SFM experiments have revealed an intermediate state for the streptavidin (or avidin)-biotin complex [38, 41]. However, since each energy barrier defines a time-scale (a range of loading rate that has to be compatible with the time-scale of the experiment) only a specific part of the energy landscape can be mapped in a typical DFS experiment [47, 48].

3.3. Experimental

DFS measurements were performed with a commercial SFM instrument using some external data acquisition and data output capabilities in addition. The spring constants of all cantilevers (ranging from 12 to 17 pN/nm) were calibrated by the thermal fluctuation method [49] with an absolute uncertainty of 20%. For the temperature measurements presented below, the temperature was controlled using a home built cell where the buffer solution that immersed both

the probe surface and the SFM cantilever was in contact with a Peltier element, driven with a constant current source. Measurements at different points of the cell showed deviations of less than 2 °C.

The preparation and immobilization of all oligonucleotides follows the protocol described in Refs. 39 and 42.

3.4. Probability distribution and specificity of rupture forces

Unbinding events are caused by thermal fluctuations rather than by mechanical instability. Therefore unbinding forces show a distribution whose width σ is mainly determined by the force scale F^0 , *i.e.* $\sigma = F^0(\Delta x)$.

When approaching the tip to the surface, many non-specific attachments may occur, even in the presence of treated surfaces or pure polymer samples. Therefore, it is imperative to test the specificity of the interaction (Fig. 7.).

Unspecific interactions can be minimized using linkers (e.g. poly(ethylene)glycol (PEG) linkers) that shift the region where unbinding takes place away from the surface. Finally, to quantify the most probable value for the unbinding force of a single complex, one has to work under conditions in which the probability that two or more duplexes are attached to the tip is low.

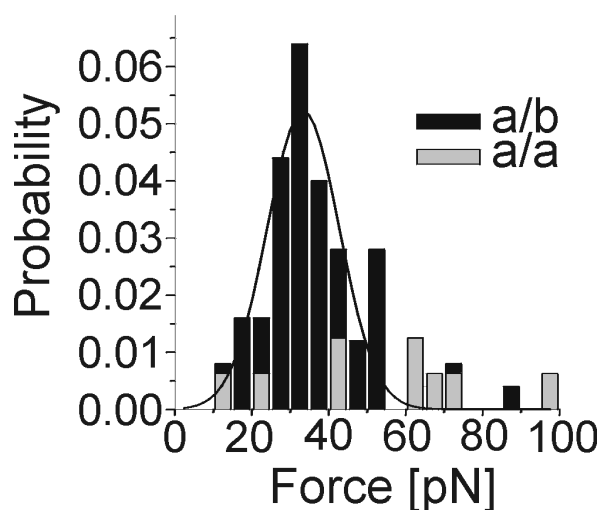


Figure 7: A typical probability distribution for the rupture force (about 500 approach/retract cycles, retract velocity 100 nm/s) [39]. For this experiment, an oligomer *a* (see text) was attached to the tip of the SFM-cantilever and its complement *b* was immobilized on the surface (complements were pulling apart at their opposite 5'-ends). Gray rectangles (*a* against *a*), black rectangles (*a* against *b*). To minimize unspecific interactions (e.g. *a* against *a*) and multiple unbinding events, 30-nm-long PEG linkers were attached to the 5'-ends. Note that the scale-force F^0 can be in principle determined from the width of the distribution.

These conditions are fulfilled for a low concentration and when the linkers have a length that is comparable to the diameter of the SFM-tip (about 50 nm). In this case, it is very unlikely that two or more linkers are extended to the same length when stretched. However, subsequent rupture events may be found. But still, the last rupture event will occur for an applied force equal to F^* .

3.5. Dynamic measurements

3.5.1. Base pair dependence

We now present DFS measurements performed on complementary DNA strands of different length [10, 20, and 30 base pairs (bp)] and pulled apart at their opposite 5'-ends. The base sequences of the oligonucleotides were designed to favor the binding to its complementary oligonucleotides in the ground state with respect to intermediate duplexes in which the strand is shifted relative to its complement. We have chosen the oligomer **a** (5'-G-G-C-T-C-C-C-T-T-C-T-A-C-C-A-C-T-G-A-C-A-T-C-G-C-A-A-C-G-G-3'), which contains 30 bases and in which every three base motive occurs only once in the sequence. For this sequence, self-complementarities are avoided because the complement of each three-base motive is not contained in the sequence. **a** was tested against its complement **b** (30 bp) and against truncated components **c** (20 bp) and **d** (10 bp), respectively.

As expected, a F^* versus $\ln(v)$ plot shows a linear behavior for each duplex (Eq. 7, see Figure 8).

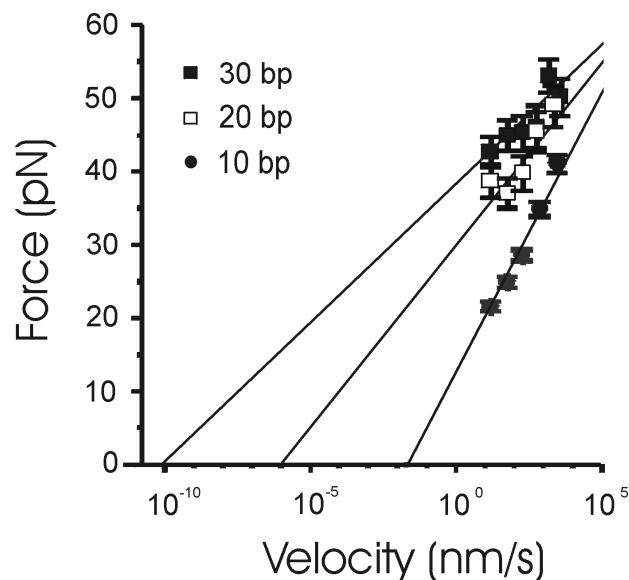


Figure 8: Velocity dependence of the most probable unbinding force [39]. Back squares (a-tip/b-surface, 30 bp), empty squares (a-tip/c-surface, 20 bp), circles (a-tip/d-surface, 10 bp). From a linear fit, both the force-scales $F^0 = k_B T / \Delta x$ and thermal off-rates can be determined.

For each duplex, the distance Δx from the ground state to the energy barrier and the thermal off rate k_{off} were determined according to Eq. 7. The Δx distance was found to follow the linear relation: $\Delta x = [(0.7 \pm 0.3) + (0.07 \pm 0.03) \times n]$ nm, where n is the number of base pairs. This increase of Δx with n clearly indicates cooperativity in the unbinding process. Measurements of k_{off} can be described by: $k_{off} \approx 10^{\alpha - \beta n} s^{-1}$, where $\alpha = 3 \pm 1$ and $\beta = 0.5 \pm 0.1$. The obtained k_{off} values are in good agreement with thermodynamical data [50]. Let us finally point out that an exponential decrease of the thermal off-rate with the number of

base pairs is expected because of the increase of the activation energy for dissociation (Eq. 5). However, the pre-factor τ_0 in Eq. 5 also strongly decreases with the number of base pairs because of the increasing number of degrees of freedom of the system.

3.5.2. Temperature dependence

In this section, temperature dependent DFS measurements are briefly discussed. The sequence **e** (5'-T-A-T-T-A-A-T-A-T-C-A-A-G-T-T-G-3') [51] attached to the tip and its complement **f** was immobilized on the surface. As previously, PEG linkers were used and DNA strands were pulled apart at their opposite 5'-ends. The specificity of the interaction was comparable to the one obtained in base-pair dependent measurements (Fig. 7).

As seen in Fig. 9, the slope of the F^* versus $\ln(r)$ plots changes as a function of temperature, which evidences for a strong temperature dependence of Δx . This result emphasizes the fact that for the DNA-duplex, the energy landscape is much more complicated than that of ligand-receptor bonds.

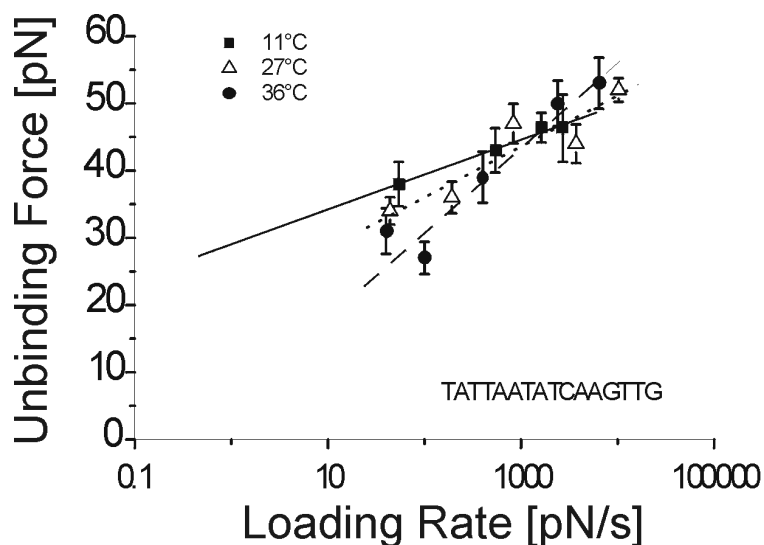


Figure 9: The most probable unbinding force as a function of the loading rate (e-tip/f-surface, 16 bp) obtained at different temperatures. Squares (11 °C), triangles (27 °C), circles (36 °C).

As a consequence, the unbinding process may involve many different reaction paths. In this case, thermal fluctuations are expected to play a key role.

3.6. Future of dynamic force spectroscopy

Using DFS measurements, the energy landscape of molecular bonds can be mapped. Moreover, relevant parameters such as the location and height of the barriers and the thermal off-rates can be determined. Our measurements confirm that the most probable force for unbinding scales as the logarithm of the loading rate. From this dependence, both the natural thermal off-rate for dissociation K_{off} and the bond length x along the reaction coordinate were

determined. Our measured K_{off} values are in agreement with bulk temperature measurements indicating the validity of our measurements. The base pairs dependent measurements indicate that unbinding of DNA strands is a cooperative process. Temperature dependent measurements evidence for a decrease of Δx as the temperature increases [42]. This behavior, which is not expected in the case of one dimensional energy landscape with a sharp energy barrier, indicates the role played by entropic contributions when unbinding DNA and unfolding RNA or proteins. However, the linear decrease of x with the temperature is still an open question. It is obvious that the exact relationship between the bond length and the temperature is not straightforward and calculations are needed to explain the observed properties. Since the limited range of loading rates available in an SFM experiment does not allow one to map the whole energy landscape, such experiments should be combined in the future with other DFS setup such as bio-membrane force probe or optical tweezers setups. An additional solution is to apply small cantilevers, which allow faster pulling and exhibit less thermal noise; so smaller unbinding forces can be detected. These small cantilevers are still experimental [52] and great efforts are being made to commercialize them in the future. These developments will also ask for instrument development so it is expected to last a few years before they are widely used. One could envision that the dynamic force spectroscopy will be applied in the future to assess the binding affinity of biomolecules on bio-arrays but the experimentalists have to catch up to step in this direction.

4. ADVANCED BIO-SENSING USING MICRO MECHANICAL CANTILEVER ARRAYS

4.1. Introduction to micro-mechanical bio-sensors

During the last few years a series of new detection methods in the field of biosensors have been developed. Biosensors are analytical devices, which combine a biologically sensitive element with a physical or chemical transducer to selectively and quantitatively detect the presence of specific compounds in a given external environment.

These new biosensor devices allow sensitive, fast and real-time measurements. The interaction of biomolecules with the biosensor interface can be investigated by transduction of the signal into a magnetic [53] an impedance [54] or a nanomechanical [55] signal. In the field of nanomechanical transduction, a promising area is the use of cantilever arrays for biomolecular recognition of nucleic acids and proteins. One of the advantages of the cantilever array detection is the possibility to detect interacting compounds without the need of introducing an optically detectable label on the binding partners. For biomolecule detection the liquid phase is the preferred one but it has been shown that the cantilever array technique is also very appropriate for

the use as a sensor for stress [56], heat [57] and mass [58]. Recent experiments showed that this technique could also be applied as an artificial nose for analyte vapors (e.g. flavors) in the gas phase [59].

4.2. Nanomechanical cantilever as detectors

The principle of detection is based on the functionalization of the complete cantilever surface with a layer, which is sensitive to the compound to be investigated. The detection is feasible in different media (e.g. liquids or gas phase). The interaction of the analyte with the sensitive layer is transduced into a static deflection by inducing stress on one surface of the cantilever due to denser packing of the molecules [60] or a frequency shift in case of dynamic detection mode [61] due to changes in mass.

4.3. Overview of the two detection modes

4.3.1. Static mode

In static mode detection, the deflection of the individual cantilever depends on the stress induced by the binding reaction of the specific compounds to the interface. The interface has to be activated in an asymmetrical manner, as shown in figure 10. Most often one of the cantilever surfaces is coated with a metallic layer (e.g. gold) by vacuum deposition techniques and subsequently activated by binding a receptor molecule directly *via* a thiol group to the interface (e.g. thiol modified DNA oligonucleotides) or as in case of protein recognition by activating the fresh gold interface with a self-assembling bi-functional bio-reactive alky-thiol molecule to which the protein moiety is covalently coupled [62].

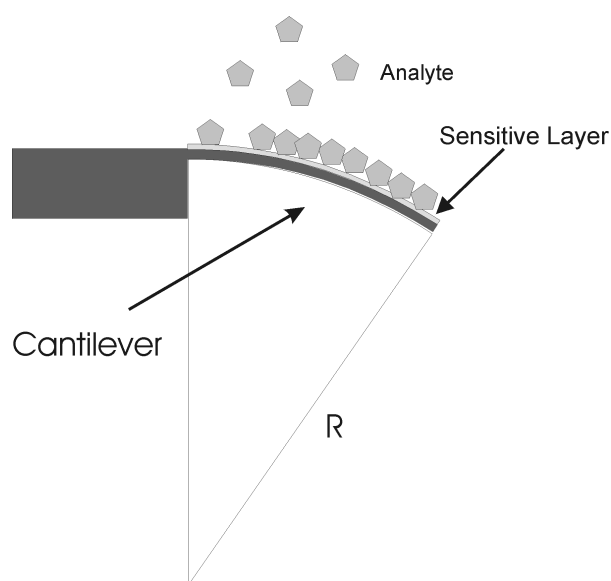


Figure 10: Interaction of the analyte (light gray pentagons) with the sensitive layer induces a stress on the interface and bends the cantilever (note the asymmetric coating of the individual cantilever surface).

The radius R of the curvature of the cantilever is given by the Stoney's law [63]

$$\sigma = Et_{\text{cant}}^2 (6R(1-\gamma))^{-1} \quad (8)$$

where σ is the stress, γ is the Poisson ratio, E the Young's Modulus and t_{cant} the thickness of cantilever. The thickness of the lever is an important parameter, which can be varied to in— or decrease the sensitivity of the device. By reducing the thickness a larger deflection due to stress change at the interface is possible. Note, that the interaction of the ligand with the receptor molecule has to occur in the vicinity of the interface. No flexible linking of the receptor molecule is allowed due to the fact that the induced stress will be diminished. IN addition the receptor molecules should be immobilized natively tightly packed on the interface to interact with the substances to be analyzed.

4.3.2. Dynamic mode

In the case of dynamic mode detection, the resonance frequency of the individual cantilever, which has to be excited, depends on the mass. The binding reaction of the analyte to the interfaces is increasing the mass and the resonance frequency is normally decreased. In figure 11 the scheme of dynamic cantilever detection is shown.

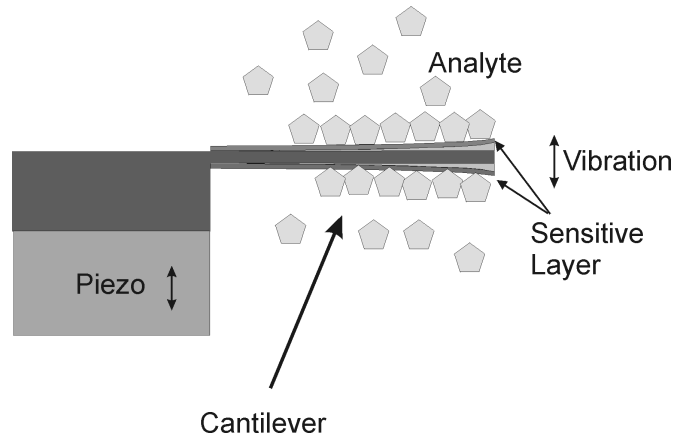


Figure 11: Interaction of analyte (light gray pentagons) with sensitive layers induces a change in the resonance frequency of cantilever.

The cantilever is excited by a piezo element. The change in mass (Δm) during the experiment due to an uptake of interacting biomolecules induces a change in the resonance frequency of cantilever, which can be described by the following formula [61]:

$$\Delta m = K(4n\pi^2)^{-1}(f_1^{-2} - f_0^{-2}) \quad (9)$$

where the resonance frequency prior and during experiment are f_0 and f_1 , K is the spring constant of cantilever and n a factor depending on the geometry

of the cantilever. The uptake of mass due to specifically interacting molecules is doubled in this manner and the cantilever does not respond to temperature changes *via* a bimetallic effect. Additionally the preparation involves fewer steps as in the case of the static detection mode [57].

4.4. Setups

At the institute of Physics in Basel at the University of Basel in collaboration with the IBM Research Laboratory Zurich we developed cantilever array setups both for static and dynamic mode operation in liquids and in the gas phase.

The principal part of the setup is an array of 8 cantilevers, produced by classical lithography technology with wet etching. A typical picture of such a cantilever array is shown in figure 12.

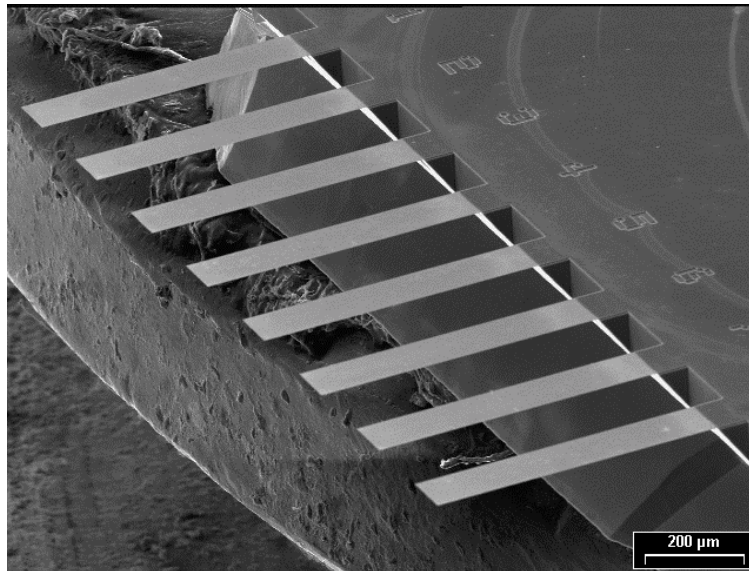


Figure 12: SEM picture of an array of 8 cantilevers. Dimensions: width 100 μm , length 500 μm , 0.5 μm with a pitch of 250 μm in-between.

The structure of an array is composed of 8 cantilevers. The etching process provides cantilever thickness ranging from 250 nm to 7 μm adapted for the individual application (*i.e.* static or dynamic mode).

A classical laser beam deflection optical detection for both the static and dynamic mode set up is used (see Fig. 13).

The laser source consists of an array of 8 VCELs (Vertical Cavity Surface Emitting Lasers, 760 nm wavelength, pitch 250 μm) and the position detection is obtained through a linear position sensitive detector (PSD). The array is mounted in a cell, which can be used for measurements in gas or a liquid environment.

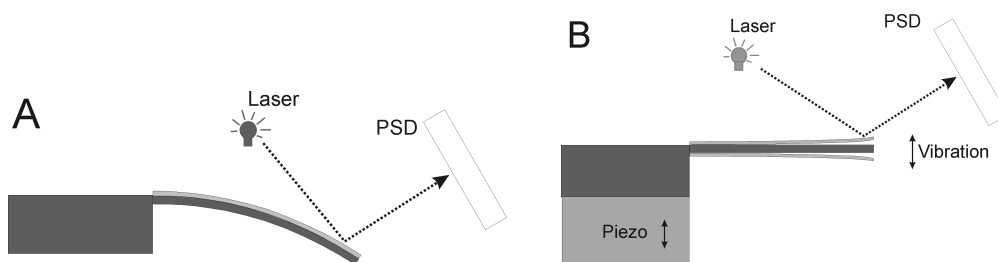


Figure 13: Optical detection used for static (A) or dynamic (B) mode detection of average cantilever position using a multiple laser source VCELS and a position sensitive device (PSD).

A scheme showing the setup is displayed in figure 14. The operation of our instruments is fully automatic. During the time course of a few hours up to eight different samples can be probed using the automatic fluid delivery. The instrumental noise of the static setup lies in the sub-nanometer range and the dynamic setup is able to detect mass changes in the order of picograms.

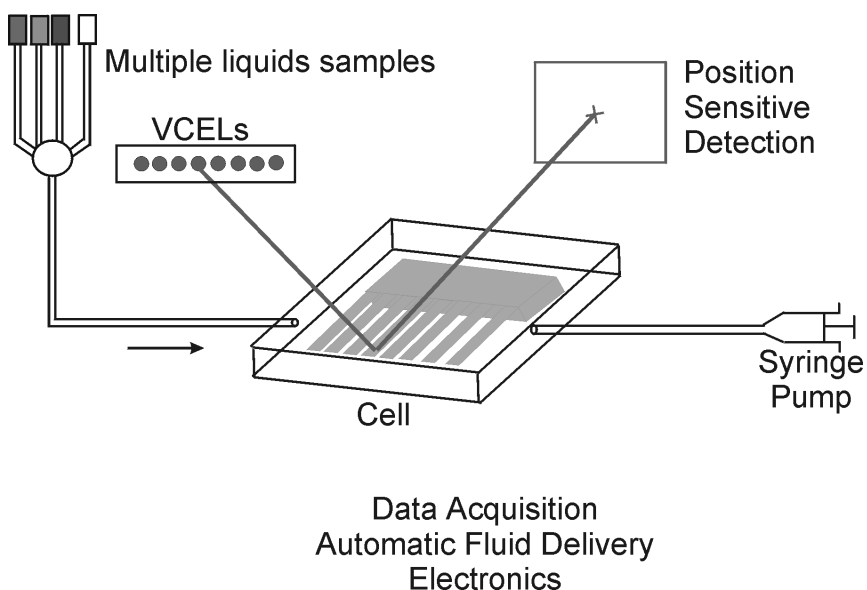


Figure 14 General structure of cantilever array setups for gas/liquid samples.

The key advantage to use cantilevers arrays is to offer the possibility of *in situ* reference and the simultaneous detection of different substances. The *in situ* reference is needed to avoid the thermo-mechanical noise especially in fluid phase detection. Changes in refractive index when the buffer changes will also contribute to a ‘virtual’ motion of the cantilever. As visible in figure 15 only the ‘real’ motion, which is the difference in-between the cantilevers on the same chip is originating from the specific biomolecular interaction.

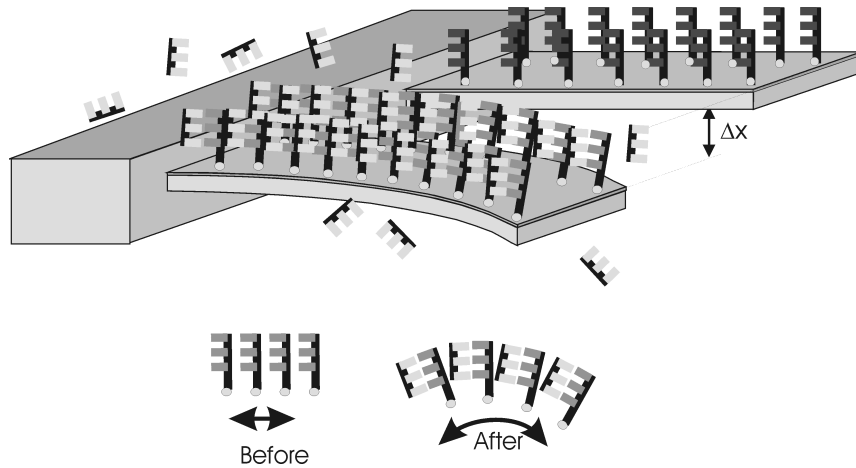


Figure 15: Static detection of biomolecular interaction. The cantilevers have to be equilibrated and then the biomolecule of interest is injected. Due to the specific interaction of the injected biomolecules (light gray) with the biomolecules on the cantilever shown in front stress builds up. A scheme is shown below. The interaction of the biomolecules with the receptor molecules induces stress at the interface, which deflects the individual cantilever specifically.

In figure 16 (A) A raw signal of the cantilever array is displayed. Since there will always be instrumental or thermal drift, the differential signal detection is mandatory. The figure shows an experiment with a set of three cantilevers (thickness ~ 500 nm). In this experiment we used two reference cantilevers with different coatings and one specific biorecognition cantilever. This cantilever is being stressed upon binding of the corresponding interacting biomolecule.

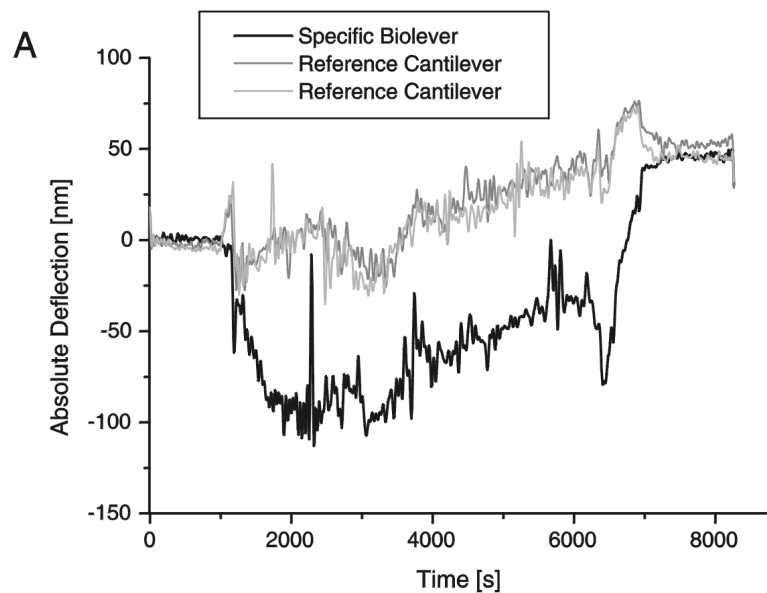


Figure 16 A: Raw data of a three-lever bio-array experiment. In the top traces (light gray, gray) the motion of the reference cantilevers is shown. In black color the motion of the biologically specific cantilever is

displayed. Upon injection of interacting biomolecules [-1000 s] turbulences of the liquid cause all levers to undergo some motion, which is stabilized immediately when the flow is stopped [-1200s]. The specific binding signal quickly builds up and remains stable. The interaction is fully reversible and can be broken by shifting the equilibrium of the binding reaction by injecting pure buffer solution [-6500s] into the fluid chamber. During the time course of two to three hours, we regularly see a drift of the cantilever arrays on the order of tens of nanometers even though the setup is temperature-stabilized (0.05°C).

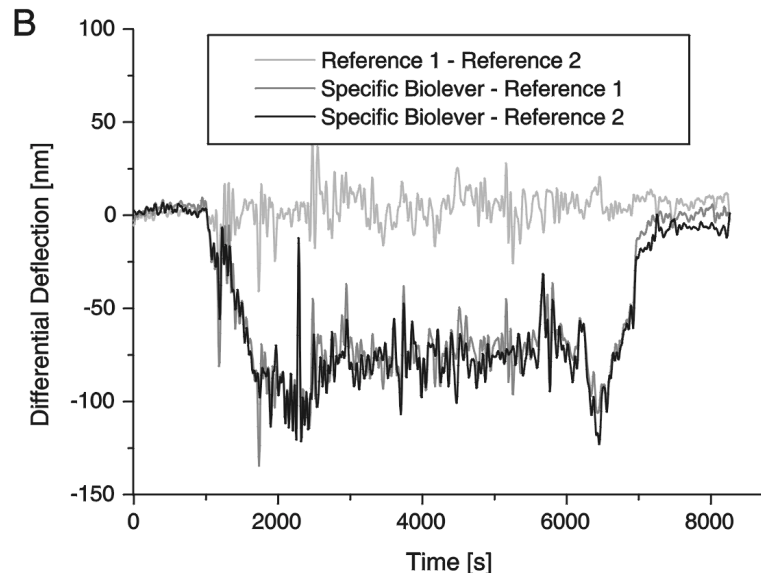


Figure 16 B: Differential data of the experimental set of figure 16 (A). The difference of in-between the two reference cantilevers is shown (light grey). Except for some small motions, no differential bending is observed, whereas in the color dark grey and black the difference of the specifically reacting cantilever with respect to the reference cantilevers is shown. As shown after ~6500s pure buffer solution is injected and the differential signal collapses to values close to the starting point where no interacting biomolecules were present in the experiment.

As visible in figure 16 (B) the differential signal lacks of any external influences except for the specific biomolecular interaction which induces a differential signal of ~90 nm relative to the *in situ* reference. The experiment is reversible and can be repeated using different concentrations of analytes. In a recent work we presented data, which allow extracting of the thermodynamics of the interacting biomolecules (*i.e.* DNA) [64]. Deflection signals as small as a few nanometers are easily detected. Currently, the detection limit in static experiments lies in the range of nanomolar concentration [64] but can be significantly lowered by using cantilever arrays of thickness in the range of 250 – 500 nm in the future.

Great care has to be taken in the selection of the internal reference lever. In the case of DNA detection an oligonucleotide displaying a sequence, which does not induce cross talk binding reactions to the sequences to be detected is chosen. Coating with thin layers of titanium and gold using vacuum deposition modifies one side of the cantilever array. Onto this metallic interface a thiol-

modified oligonucleotide self-assembles in a high-density layer. Complementary and unknown oligonucleotide sequences are then injected and the specific interaction is directly visible within minutes. Stress at the interface is built up due to a higher density of packing (see figure 15). In protein detection, a protection of the asymmetrically coated cantilever has to be considered. Preparation of protein detecting cantilevers is a multi step procedure and requires surface chemistry knowledge. The side opposite to the biomolecular-modified side is generally protected by a poly-ethylene-glycol (PEG) layer. The bio-reference surface can be coated by using unspecifically interacting proteins (e.g. bovine serum albumin). In protein detection experiments larger 'fluctuations' of the cantilevers are observed (e.g. figure 16) than in the ssDNA-ssDNA experiments. A possible interpretation of this difference might be due to the fact that the proteins used [μM] absorb light within the visible spectrum and therefore induce some local changes in index of refraction. Specific signals are normally measured within minutes without problems. Usually some drift of few tens of nanometers is observed of the complete set of cantilevers during the time course of the experiment even though the instruments temperature is stabilized within ± 0.05 °C. But these effects are completely eliminated by using a differential read out on the very same cantilever array.

Cantilevers arrays are already applied as detector both in static and dynamic mode [60, 61]. Recent articles show the potential for detection of DNA hybridization [55, 64], cell capture or toxin detection [53]. Integrating cantilever arrays into micro-fluidic channels will significantly reduce the amount of sample required [65]. Attempts have been made to get data from single cantilever experiments for DNA [66] or antibody antigen reaction [67] or from a two-cantilever setup using different stiffness for the individual cantilevers [68]. We would like to point out that these approaches have serious drawbacks. Information extracted from these experiments, which often last multiple hours, cannot exclude unspecific drift of any kind. The signal in these experiments is interpreted as specificity on the biomolecular level but no correlation from one lever to the next is applicable if only one lever is used at the time. In a second approach, cantilevers with different stiffness are used to monitor the nanometer motions. Since the individual cantilever used show a difference of factor four in terms of stiffness, the response, which originates from specific interaction, is difficult to extract. The sensitivity of this approach is hampered due to the differences in stiffness, which is directly correlated to the thickness of the cantilever used (see Eq. 8). An interaction of the biomolecule with the stiffer reference cantilever might not be detectable if the stress signal lies within the thermal noise of that lever.

4.5. Future applications of cantilever arrays

The cantilever array technology explore a wide area of applications; all biomolecular interactions are in principle able to be experimentally detected using cantilever array as long as mass change or surface stress is induced due to the specific interaction. A few applications so far demonstrated promising results in the field of biological detection. The cantilever based sensor platform might fill the gap between the very expensive analytical instrumentation (e.g. mass-spectroscopy, HPLC, SPR), which are sensitive but costly and relatively slow and the chip technologies (e.g. gene-arrays) with its advantage of easy multiplexing capabilities, but the need of fluorescence labeling and with its restriction to higher molecular weight compounds like proteins and nucleic acids so far.

In comparison to the methods described above, the cantilever technology is cheap, fast, sensitive and applicable to a broad range of compounds. The cantilever arrays can be used repeatedly for successive experiments. The lack of multiplexing could be overcome by the application of large cantilever arrays with > 1000 Cantilevers/chip. There are now projects launched to introduce commercial platforms providing arrays of eight cantilevers for applications in the liquid or in the gas phase. A critical point for future developments in this field will be the access to the cantilevers arrays as it is in the 'normal' field biological applications using single cantilever scanning force microscopy. At the moment, there are no biological experiments published which use the dynamic mode detection. But as we believe the ease of preparation (symmetrically as pointed out above) and the fact that the sensitivity towards environmental changes is reduced, this might be the instrumental approach of choice for the future biological detection using cantilever arrays.

5. CONCLUSION

During the last decade single molecule experiments provided ample information in the field of biological basic research. We would like to point out again that these kinds of experiments do not probe an ensemble of molecules and therefore give access to information or properties of sub-populations of biomolecules. These experiments don't have to be synchronized and therefore no averaging occurs. In nature many cases, which define the status of an organism are depending on properties or activity of individual sub-populations (e.g. start of cancer in an individual cell). — It is a long way to go to have real implications of single molecule manipulation experiments on daily life, but the information revealed so far, show that the clues to some specific biological problems might lie in the detail [e.g. Ref. 22]. In addition, it is important to mention that single molecule experiments are always technically most demanding and the future results obtained on single molecule will mainly depend on instrumentation capabilities. One 'drawback' of single molecule

experiments is, that one experiment is not sufficient to elucidate the properties of a subpopulation. Enough experimental data has to be gathered, which is time consuming, to allow applying statistics.

A way out might be to combine the high sensitivity of these force measuring devices and sample a few thousand molecules at a given time as it is done by using cantilever arrays. This new array technology is not limited to genomic studies but can also detect protein-protein interactions [55], and will thus find applications in the fields of proteomics, biodiagnostics and combinatorial drug discovery where rapid, quantitative binding measurements are vital. The ability to directly translate biochemical recognition into nano-mechanical motion might have wide ranging implications, for example DNA computing applications or nanorobotics. The Nano-Newton forces generated are sufficient to operate micromechanical valves or microfluidic devices and *in situ* delivery devices could be triggered directly by signals from gene expression, immune response or single cells.

ACKNOWLEDGEMENT

Financial support of the NCCR "Nanoscale Science" the Swiss National Science Foundation and the ELTEM Regio Project Nanotechnology is gratefully acknowledged. We would like to thank our colleagues from Basel and IBM Rüschiikon for the great collaborative effort and for their valuable contributions to make progress in the field single molecules manipulation using OT and SFM and in the field of cantilever arrays. We are especially grateful to Ernst Meyer, Peter Vettiger, Felice Battiston, Torsten Strunz, Irina Schumakovitch and Hans-Joachim Güntherodt.

REFERENCES

- [1] A. Engel and D.J.Müller, *Nature Struct. Biol.*, 7 (2000) 715.
- [2] M. Guthold, X.S. Zhu, C. Rivetti, G.L. Yang, N.H. Thomson, S. Kasas, H.G. Hansma, B. Smith, P.K. Hansma and C. Bustamante, *Biophys. J.*, 77 (1999) 2284.
- [3] M. Rief, M. Gautel, F. Oesterhelt, J.M. Fernandez, and H.E. Gaub, *Science*, 276 (1997) 1109.
- [4] A. Ashkin, *Phys. Rev. Lett.*, 24 (1970) 156.
- [5] A. Ashkin, J.M. Dziedzic, J.C. Bjorkholm and S. Chu, *Opt. Lett.*, 11 (1986) 288.
- [6] A. Ashkin and J.M. Dziedzic, *Science*, 235 (1987) 1517.
- [7] A. Ashkin, J.M. Dziedzic and T. Yamane, *Nature*, 330 (1987) 769.
- [8] K. Svoboda and S.M. Block, *Annu. Rev. Biophys. Biomol. Struct.*, 23 (1994) 247.
- [9] N. Pam and H.M. Nussenzveig, *Eur. Phys. Lett.*, 50 (2000) 702.
- [10] K.C. Neuman, E.H. Chadd, G.F. Lion, K. Bergman and S.M. Block, *Biophys. J.*, 77 (1999) 2856.
- [11] G. Leitz, E. Fällman, S. Tuck and Ove Axner, *Biophys. J.*, 82 (2002) 2224.
- [12] R.S. Afzal and E.B. Treacy, *Rev. Sci. Instrum.*, 63 (1992) 2157.
- [13] S.B. Smith, PhD. Thesis, University of Twente, The Netherlands 1998.

- [14] W. Grange, S. Husale, H.J. Güntherodt and M. Hegner, *Rev. Sci. Instrum.*, in press (June 2002).
- [15] F. Gittes and C.F. Schmidt, *Eur. Biophys. J.*, 27 (1998) 75.
- [16] M.B. Viani, T.E. Schaffer, A. Chand, M. Rief, H.E. Gaub, P.K. Hansma, *J. Appl. Phys.*, 86 (1999) 2258.
- [17] A.D. Metha, M. Rief, J.A. Spudich, D.A. Smith and R.M. Simmons, *Science*, 283 (1999) 1689.
- [18] C. Bustamante, J.C. Macosko and G.J.L. Wuite, *Nat. Rev., Mol. Cell Biol.*, 1 (2000) 130.
- [19] G. Woehlke and M. Schliwa, *Nat. Rev., Mol. Cell Biol.*, 1 (2000) 50.
- [20] G.J. Wuite, S.B. Smith, M. Young, D. Keller and C. Bustamante, *Nature*, 404 (2000) 103.
- [21] R.J. Davenport, G.J. Wuite, R. Landick and C. Bustamante, *Science*, 287 (2000) 2497.
- [22] D.E. Smith, S.J. Tans, S.B. Smith, S. Grimes, D.L. Anderson and C. Bustamante, *Nature*, 413 (2001) 748.
- [23] S.B. Smith, Y. Cui and C. Bustamante, *Science*, 271 (1996) 795.
- [24] M.S. Kellermayer, S.B. Smith, H.L. Granzier and C. Bustamante, *Science*, 276 (1997) 1112.
- [25] L. Tskhovrebova, J. Trinick, J.A. Sleep, and R.M. Simmons, *Nature*, 387 (1997) 308.
- [26] J. Liphardt, B. Onoa, S. B. Smith, I. Tinoco Jr. and C. Bustamante, *Science*, 292 (2001) 733.
- [27] M. Hegner, S.B. Smith and C. Bustamante, *Proc. Natl. Acad. Sci. USA*, 96 (1999) 10109.
- [28] S. Husale, W. Grange and M. Hegner, *Single Mol.*, (2002) in press (June 2002).
- [29] G. U. Lee, L. A. Chrisley and R. J. Colton, *Science*, 266 (1994) 771.
- [30] G. U. Lee, D.A. Kidwell and R. J., Colton, *Langmuir*, 10 (1994) 354.
- [31] V.T. Moy, E.L. Florin and H.E. Gaub, *Science*, 266 (1994) 257.
- [32] U. Dammer, O. Popescu, P. Wagner, D. Anselmetti, H.-J. Güntherodt, and G.N. Misevic, *Science*, 267 (1995) 1173.
- [33] P. Hinterdorfer, W. Baumgartner, H.J. Gruber, K. Schilcher and H. Schindler, *Proc. Natl. Acad. Sci USA*, 93 (1996) 3477.
- [34] U. Dammer, M. Hegner, D. Anselmetti, P. Wagner, M. Dreier, W. Huber and H.-J. Güntherodt, *Biophys. J.*, 70 (1996) 2437.
- [35] S. Allen, X.Y. Chen, J. Davies, M.C. Davies, A.C. Dawkes, J.C., Edwards, C.J. Roberts, J. Sefton, S.J.B. Tendler and P.M. Williams, *Biochemistry*, 36 (1997) 7457.
- [36] P.E. Marszalek, H. Lu, H.B. Li, M. Carrion-Vazquez, A.F. Oberhauser, K. Schulten and J.M. Fernandez, *Nature*, 402 (1999) 100.
- [37] R. Ros, F. Schwesinger, D. Anselmetti, M. Kubon, R. Schäfer, A. Plückthun and L. Tiefenauer, *Proc. Natl. Acad. Sci USA*, 95 (1998) 7402.
- [38] R. Merkel, P. Nassoy, A. Lueng, K. Ritchie and E. Evans, *Nature*, 397 (1999) 50.
- [39] T. Strunz, K. Oroszlan, R. Schäfer and H.-J. Güntherodt, *Proc. Natl. Acad. Sci USA*, 96 (1999) 11277.
- [40] F. Schwesinger, R. Ros, T. Strunz, D. Anselmetti, H.-J. Güntherodt, A. Honegger, L. Jermutus, L. Tiefenauer and A. Plückthun, *Proc. Natl. Acad. Sci USA*, 97 (2000) 7402.
- [41] R. De Paris, T. Strunz, K. Oroszlan, H.-J. Güntherodt, and M. Hegner, *Single Mol.*, 1 (2000) 285.
- [42] I. Schumakovitch, W. Grange, T. Strunz, P. Bertoncini, H.-J. Güntherodt and M. Hegner, *Biophys J.*, 82 (2002) 517.
- [43] E. Evans, A. Leung, D. Hammer and S. Simon, *Proc. Natl. Acad. Sci USA*, 98 (2001) 3784.
- [44] H.A. Kramers, *Physica Utrecht*, 7 (1940) 284.
- [45] I. Bell, *Science*, 200 (1978) 618.

- [46] E. Evans, *Annu. Rev. Biophys. Biomol. Struct.*, 30 (2001) 105.
- [47] E. Galligan, C.J. Roberts, M.C. Davies, S.J.B. Tendler and P.M. Williams, *J. Chem. Phys.*, 114 (2001) 3208.
- [48] B. Heymann and H. Grubmüller, *Phys. Rev. Lett.*, 84 (2000) 6126.
- [49] J.L. Hutter and J. Bechhoefer, *Rev. Sci. Instrum.*, 64 (1993) 1868.
- [50] D. Pörschke and M. Eigen, *J. Mol. Biol.*, 62 (1971) 361.
- [51] N. Tibanyenda, S. H. Debruin, C.A.G. Haasnoot, G. A. Vandermarel, J. H. Vanboom, C. W. Hilbers, *Europ. J. Biochem.*, 139 (1984) 19.
- [52] M.B. Viani, T.E. Schaffer, G.T. Paloczi, L.I. Pietrasanta, B.L. Smith, J.B. Thompson, M. Richter, M. Rief, H.E. Gaub, K.W. Plaxco, A.N. Cleland, H.G. Hansma and P.K. Hansma, *Rev. Sci. Instr.*, 70 (1999) 4300.
- [53] D.R. Baselt, G.U. Lee and R.J. Colton, *Vac. Sci. Technol. B*, 14(2) (1996) 789.
- [54] H. Masayuki, Y. Yoshiaki, T. Hideki, O. Hideo, N. Tsunenori and Jun M., *Biosensors and Bioelectronics* 17 (2002) 173.
- [55] J. Fritz, M.K. Baller, H.P. Lang, H. Rothuizen, P. Vettiger, E. Meyer, H.-J. Güntherodt, Ch. Gerber and J.K. Gimzewski, *Science*, 288 (2000) 316.
- [56] R. Berger, E. Delamarche, H.P. Lang, Ch. Gerber, J.K. Gimzewski, E. Meyer and H.-J. Güntherodt, *Science*, 276 (1997) 2021.
- [57] R. Berger, Ch. Gerber, J.K. Gimzewski, E. Meyer and H.-J. Güntherodt, *Appl. Phys. Lett.*, 69 (1996) 40.
- [58] T. Bachels, R. Schäfer and H.-J. Güntherodt, *Phys. Rev. Lett.*, 84 (2000) 4890.
- [59] M.K. Baller, H.P. Lang, J. Fritz, Ch. Gerber, J.K. Gimzewski, U. Drechsler, H. Rothuizen, M. Despont, P. Vettiger, F.M. Battiston, J.P. Ramseyer, P. Fornaro, E. Meyer and H.-J. Güntherodt, *Ultramicroscopy*, 82 (2000) 1.
- [60] J. Fritz, M.K. Baller, H.P. Lang, T. Strunz, E. Meyer, H.-J. Güntherodt, E. Delamarche, Ch. Gerber and J.K. Gimzewski, *Langmuir*, 16 (2000) 9694.
- [61] F.M. Battiston, J.P. Ramseyer, H.P. Lang, M.K. Baller, Ch. Gerber, J.K. Gimzewski, E. Meyer and H.-J. Güntherodt, *Sensors and Actuators B*, 77 (2001) 122.
- [62] P. Wagner, M. Hegner, P. Kern, F. Zaugg and G. Semenza, *Biophys. J.* 70 (1996) 2052.
- [63] G.G. Stoney, *Proc. R. Soc. London Soc. A* 82 (1909) 172.
- [64] R. McKendry, T. Strunz, J. Zhang, Y. Arntz, M. Hegner, H. P. Lang, M. Baller, U. Certa, E. Meyer, H.-J. Güntherodt and Ch. Gerber, *Proc. Natl. Acad. Sci. USA* (2002) in press.
- [65] J. Thaysen, R. Marie and A. Boisen, in *IEEE Int. Conf. Micro. Electro. Mech. Syst.*, Tech. Dig. Publisher: Institute of Electrical and Electronic Engineers, New York, 14th (2001) 401.
- [66] K.M. Hansen, H.F. Ji, G.H. Wu, R. Datar, R. Cote, A. Majumdar and T. Thundat, *Anal. Chem.* 73 (2001) 1567.
- [67] G.H. Wu, R.H. Datar, K.M. Hansen, T. Thundat, R.J. Cote and A. Majumdar, *Nature Biotech.* 19 (2001) 856.
- [68] C. Grogan, R. Raiteri, G.M. O'Connor, T.J. Glynn, V. Cunningham, M. Kane, M. Charlton and D. Leech, *Biosens. Bioelectron.* 17 (2001) 201.